International Journal of Pharmaceutics 409 (2011) 185–193

Contents lists available at ScienceDirect

International Journal of Pharmaceutics

journal homepage: www.elsevier.com/locate/ijpharm

Doxorubicin loading and eluting characteristics of bioresorbable hydrogel microspheres: In vitro study

Lihui Weng, Hung C. Le, Jingying Lin, Jafar Golzarian*

Department of Radiology, University of Minnesota, Minneapolis, MN 55455, United States

ARTICLE INFO

Article history:
Received 3 November 2010
Received in revised form 23 February 2011
Accepted 26 February 2011
Available online 4 March 2011

Keywords:
Doxorubicin
Ion exchange
Bioresorbable
Hydrogel microspheres

ABSTRACT

Non-bioresorbable drug eluting microspheres are being increasingly used for the treatment of unresectable liver tumors, whereas bioresorbable microspheres have not received much attention. In this study, bioresorbable microspheres prepared from chitosan and carboxymethyl cellulose were loaded with doxorubicin (Doxo) via ion-exchange interactions with carboxylic groups in the microspheres. With a 25–40% decrease in the microsphere size depending on their size ranges, the microspheres could load a maximum of 0.3–0.7 mg Doxo/mg dry spheres. As confirmed by confocal microscopy, Doxo was mainly concentrated in the outer 20 ± 5 μm surface layer of the microspheres. The loaded microspheres were stable in aqueous dispersions without aggregation for a prolonged period of time but degradable in a lysozyme solution. Furthermore, the loaded microspheres exhibited a noticeable pH-sensitive behavior with accelerated release of Doxo in acidic environment due to the protonation of carboxylic groups in the microspheres. Compared to commercial non-resorbable drug eluting beads, the loaded bioresorbable microspheres showed a sustained release manner in phosphate buffered saline (PBS). The release data were fitted to an empirical relationship, which reveals a non-Fickian transport mechanism ($n = 0.55$–0.59). These results demonstrate that the bioresorbable microspheres are promising as attractive carriers for Doxo.

1. Introduction

Hepatocellular carcinoma (HCC), is the most common primary malignant tumor of the liver. It currently represents approximately 6% of all newly diagnosed cases of cancer worldwide (Lewis et al., 2006). Transarterial chemoembolization (TACE) is the most widespread available palliative treatment, which involves the injection of a chemotherapeutic agent followed by an embolic material into the hepatic artery. The embolic agent will occlude the arterial blood supply to the tumor, resulting in an infarct and subsequently necrosis of the tumor (Kettenbach et al., 2008). However, there is no standard procedure for TACE since there are so many variables. Besides, when administered at high dose systematically, most anticancer drugs can cause severe toxicity to the body, including myelosuppression, nausea, mucositis, hair loss, vomiting, and even irreversible cardiac toxicity (Bibby et al., 2005). With the traditional TACE, it is difficult to control the contact time of cancer cells and the chemotherapeutic agents without damaging the hepatic microcirculation. More importantly, it is also hard to predict the release of the chemotherapeutic agent over time. It is reported that drug-eluting beads would enable a more reproducible procedure for TACE of hepatomas (Parkin et al., 2005) due to achievable high concentrations and prolonged drug release in the tumors. Currently, in the United States, the only commercially available drug-eluting bead is the non-bioresorbable DC bead (Biocompatibles, UK), composed of PVA based hydrogel (Lewis et al., 2007). Another nonresorbable drug eluting beads available in Europe and Japan is Quadrasphere™ microsphere (Lee et al., 2010) (BioSphere Medical, Inc., MA). The rationale for bioresorbable drug eluting microspheres is to embolize the artery and release chemotherapeutic agent to the tumor only during its healing process. Meanwhile, the mass and mechanical strength of the microspheres decrease with time, and the component material will be gradually absorbed by the surrounding tissue. Moreover, bioresorbable microspheres would render subsequent access for administration of chemotherapy with respect to the cell cycle (Tsochatzis et al., 2010). Altogether, bioresorbable microspheres enable longer-term delivery of drugs to the surrounding tissue and tumor internal reservoir and abolish the need for a second surgery to remove the device.

There is currently no commercial resorbable drug eluting beads available. Hence, our group has developed a series of bioresorbable microspheres from oxidized carboxymethyl cellulose and carboxymethyl chitosan (OCMC/CCN microspheres) for

* Corresponding author at: Department of Radiology, University of Minnesota. Mayo B228, 420 Delaware Street SE, Minneapolis, MN 55455, United States. Tel.: +1 612 625 5147; fax: +1 612 626 5580.
E-mail address: jafar@umn.edu (J. Golzarian).

0378-5173/$ – see front matter © 2011 Elsevier B.V. All rights reserved.
doi:10.1016/j.ijpharm.2011.02.058

transcatheter embolization (Weng et al., 2010). The results have demonstrated that the microspheres are compressible, biodegradable and injectable. Besides, the microspheres can load dye due to the existence of the functional groups on the microsphere matrix. It is also anticipated that the functional groups on the microsphere can bind with therapeutic drugs. Doxorubicin (Doxo), is the most used effective anticancer drug in current oncological chemotherapy. Although it has high antitumor activity for the treatment of a number of solid tumors, such as bladder, gastric and hepatocellular cancers, similar to most anticancer drugs, Doxo exhibits severe side effects when administered at high dose systematically (Guhagarkar et al., 2010; Hruby et al., 2005). Therefore, some efforts have been made to deliver Doxo to targeted tissue by microspheres (Vinchon-Petit et al., 2010; Liu et al., 2001; Tan et al., 2005), micelles (Hruby et al., 2005; Kim et al., 2010; Ye et al., 2008), nanoparticles (Guhagarkar et al., 2010; Qia et al., 2010; Dreis et al., 2007) or synthetic conjugates (Greenwald et al., 2003; Karki and Ostovi, 2004) while minimizing the systemic exposure of the drug. Among various methods, microspheres with charges can load ionic drugs such as Doxo easily by a simple absorption method and show the highest loading for Doxo (Liu et al., 2001). In this work, hydrogel microspheres made of carboxymethyl cellulose and chitosan were used as a vehicle to load and release Doxo. The kinetics of loading and eluting of the microspheres with Doxo have been investigated. The results will provide useful information for the potential application of the bioresorbable CMC/CCN microspheres as a controlled release device for anticancer drugs that can presumably reduce the systematic exposure of Doxo.

2. Materials and methods

2.1. Materials

Chitosan (≥75% deacetylated), sodium carboxymethyl cellulose (M_w = ~700,000), and chicken white lysozyme were purchased from Sigma–Aldrich (St. Louis, MO). Doxorubicin stock solution (2 mg/mL) was obtained from Teva Pharmaceuticals (CA).

2.2. Methods

2.2.1. Preparation of OCMC/CCN microspheres

OCMC was first prepared by our previous method (Weng et al., 2010). In brief, 1 g sodium carboxymethyl cellulose (M_w = ~700,000, Sigma–Aldrich, St. Louis, MO) and 80 mL distilled water were added into a 250 mL flask. After complete dissolution of carboxymethyl cellulose, desired amount of sodium periodate (10%, 25%, and 50% theoretical oxidation degree, as coded OCMC-I, OCMC-II, and OCMC-III, respectively) in distilled water was added into the flask. The reaction was allowed to proceed for 24 h at 25 °C. Then ethylene glycol was added to terminate the reaction. The resulting pre-product was dialyzed with distilled water for 3 days, followed by lyophilizing. The introduction of aldehyde groups was confirmed by treating the product with tert-butyl carbazate followed by ^{1}H NMR (Ito et al., 2007).

CCN was prepared from chitosan (≥75% deacetylated, Sigma–Aldrich, St. Louis, MO) with a method described previously (Chen and Park, 2003). Briefly, into a 3-neck flask, 5 g chitosan, 20 g NaOH, 20 mL distilled water, and 80 mL isopropanol were added. After 24 h, 15 g monochloroacetic acid in 20 mL isopropanol was added. The reaction was allowed to proceed for another 4 h at 50 °C. Then 80 mL ethanol was added into the mixture to stop the reaction. The preproduct was rinsed with 70–90% ethanol to remove salt followed by vacuum drying at room temperature.

OCMC/CCN microspheres were prepared by a modified inverse emulsion-crosslinking method in the presence of a surfactant. Briefly, a CCN aqueous solution of 2 wt% (5 mL) was first mixed with 5 mL OCMC aqueous solution of 2 wt%, which was then added into 50 mL mineral oil containing 1% (v/v) Span 80, to form an emulsion with stirring. The resulting aqueous phase was allowed to evaporate over night at 45 °C with constant stirring. The sediment was isolated by precipitating in isopropanol, followed by centrifugation to remove the oil phase. The resulting microspheres were thoroughly washed with acetone and hexane before vacuum drying. The microspheres prepared from CCN with OCMC in different theoretical degrees of 10%, 25%, and 50% were coded as MS-I, MS-II, and MS-III, respectively.

2.2.2. Swelling of OCMC/CCN microspheres

The swelling of the microspheres was carried out in normal saline. To ensure complete equilibration, dry microspheres (weight = W_{dry}) were allowed to swell for 24 h at 37 °C. Excess liquid drops adhered on the surface were removed by blotting and the swollen microspheres were weighed (W_{wet}). The swelling ratio q was calculated as:

$$q = \frac{W_{wet}}{W_{dry}}. \quad (1)$$

2.2.3. Preparation of Doxo loaded microspheres

The loading of Doxo to the microspheres was performed by immersing the microspheres in a Doxo solution (0.25, 0.5, 0.75, 1, and 2 mg/mL). Briefly, 150 mg swollen microspheres (in normal saline) were added into a 20 mL glass vial, and the excess normal saline was removed as much as possible using a syringe with a 20 G needle before loading. Then 10 mL Doxo solution was added into the vial. The vial was kept at 5 °C in dark during the loading procedure. The change in the drug concentration in the loading solution was monitored by measuring the absorbance at 483 nm at time intervals 5 min, 10 min, 20 min, 30 min, 45 min, 1 day, and 2 day using a UV–visible spectrophotometer (Beckman, DU650) and comparing to a standard curve constructed from Doxo solutions with known concentrations.

2.2.4. Microscopy

The changes in the microsphere size and color during the loading procedure were monitored with a microscope (Nikon) connected to a CCD camera. Fluorescent microscope imaging of the loaded microspheres was conducted with a Zeiss Microscope interfaced with a SPOT camera. Confocal microscopy was performed with an Olympus FluoView FV1000 inverted microscope using Argon 488 nm laser.

2.2.5. Release studies of Doxo from the loaded microspheres

The release of Doxo from the microspheres was conducted in normal saline (pH = 6), acetate buffer (pH = 5.2), PBS (phosphate buffered saline, pH = 7.4), and deionized water, respectively. Briefly, loaded microspheres (3 mg) were added into a disposable plastic cuvette, and then 2 mL releasing medium was added. The concentration of Doxo released in the medium was monitored by measuring the absorbance at 483 nm as described above. The releasing was done at room temperature or 37 °C in dark with and without refreshing the medium. For the experiment with medium replaced, the medium was changed on day 1, day 3, day 6, day 12, day 19, and day 26. The drug releasing was compared to those of the commercial drug eluting beads, DC beads (Biocompatibles, UK).

2.2.6. Enzymatic degradation of the microspheres

The degradation experiment was performed in a lysozyme solution. Briefly, lysozyme was dissolved in 0.01 M PBS solution

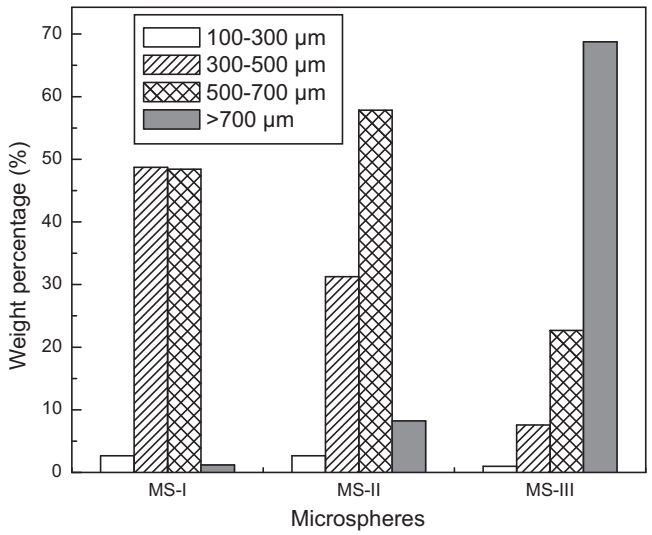

Fig. 1. Size distribution of MS-I, MS-II, MS-III.

(pH = 7.4) to form a 4 mg/mL lysozyme solution. Unloaded microspheres or Doxo loaded microspheres (2 mg) were added into a 1.5 mL plastic tube, where 0.5 mL of 4 mg/mL lysozyme was added. The tube was kept in 37 °C with mild shaking. The time of breakage and disappearance of the microspheres were noted by examination with an optical microscope.

3. Results and discussion

3.1. Preparation of OCMC/CCN microspheres

OCMC/CCN microspheres were prepared with an inverse emulsion crosslinking method which involves two steps: (1) conversion of the OCMC/CCN mixture solution into spherical micelles in the presence of surfactant. (2) The crosslinking formation between OCMC and CCN while water was removed from the system (Weng et al., 2010). The resulting microspheres are round in shape with a size ranging from 100 μm to 1000 μm. Microspheres with a narrow size distribution can be obtained by sieving, as shown in Fig. 1. The sizes of MS-I and MS-II are mainly in the range of 300–700 μm while 69% of MS-III is bigger than 700 μm, which is attributed to the formation of bigger droplets due to the increase of the viscosity of the reaction mixture with increasing the amount of functional groups in the emulsion during the preparation procedure (Agnihotri and Aminabhavi, 2006). The mean diameters are 540 ± 50, 580 ± 60, 830 ± 60 μm for MS-I, MS-II, and MS-III, respectively. With an increase in the theoretical oxidation degree of OCMC from 10% (OCMC-I) to 50% (OCMC-III), corresponding to an increase in the crosslinking density of the microspheres, the swelling ratios of the microspheres decreased from 10 to 8, while the degradation time increased from 14 days to 88 days, as summarized in Table 1.

3.2. Doxo loading into microspheres

Due to the existence of carboxylic groups (COO^-) on the hydrogel network of the microspheres, and a slightly basic nature of Doxo (pK_a = 8.2) (Kim et al., 2009), the microsphere can take up Doxo from the Doxo solution. Fig. 2 shows the uptake of Doxo by the OCMC/CCN microspheres over time 45 s, 10 min, and 45 min. Fig. 2A presents the microspheres before loading. At 45 s, the surface of microspheres slightly turned into red, while the interior of the microsphere remains intact (Fig. 2B). At 10 min, the red color of the Doxo solution surrounding the microspheres was clearly seen to become lighter, while the microspheres are redder (Fig. 2C). After 45 min, the red color of the Doxo solution was nearly depleted and the microspheres show a very bright red color (Fig. 2D). As the pH of the Doxo solution is in the range of 2.5–4.5, the amino group of Doxo is protonated. Protonated amino groups of Doxo replaced the sodium ion (Na^+) in the microsphere matrix to form $–COO^-NH_4^+$, resulting in a release of NaCl. Therefore, the interaction between Doxo and OMC/CCN microspheres is based on ion exchange, similar to the interaction mechanism between DC beads and Doxo (Lewis et al., 2007).

Fig. 3A depicts the Doxo loading dynamics of 100–300, 300–500, 500–700, and 700–850 μm MS-II in a 2 mg/mL Doxo solution. First, the drug was taken-up into the beads very rapidly for the first 2 h and then leveled off. The smaller the microspheres, the higher the loading speed in the first 2 h. Furthermore, the maximum loading is around 0.3–0.7 mg Doxo per mg dry spheres depending on the size of the microspheres. The rate of drug loading for smaller microspheres was faster than for bigger ones. This effect has been observed previously for DC beads, which is attributed to the increased surface area with a decrease in the microsphere diameter (Lewis et al., 2007). As mentioned above, there are plenty of negative charges on the polymer network of OCMC/CCN microspheres. Upon binding with Doxo, the net negative charges of the microspheres will decrease, leading to a less impulsion force inside the polymer network of the microspheres. As expected, the microspheres shrink during the loading process. Fig. 3B shows the dependence of the size of microspheres in four different sizes on the loading time. Upon maximum loading, the microspheres exhibit a 25–40% decrease in their sizes. In addition, it is reported that Doxo tends to self associate through π–π stacking interactions of the anthracycline rings (Karki and Ostovi, 2004; Kim et al., 2009; Cheung et al., 2004). This interaction will form hydrophobic area which also contributes to the water reduction of the microsphere, resulting in shrinkage of the microspheres (Lewis et al., 2007).

The loading amount of Doxo to the microspheres was found to increase with an increase in the Doxo concentration, as shown in Fig. 3C. For instance, the Doxo loaded increased from 0.014 mg/wet microsphere to 0.075 mg/mg wet microsphere when the concentration of Doxo solution increased from 0.5 mg/mL to 2 mg/mL. In a 2 mg/mL Doxo solution, the maximum loading of MS-I, MS-II, and MS-III were 0.066, 0.075, 0.077 mg/mg wet microspheres, as summarized in Table 1. The Doxo loaded microspheres prepared under these conditions were stable in normal saline, exhibiting no aggregation for a prolonged period of time (up to 5 months). It is worth noting that the Doxo loading was performed with a clinically preferred soaking method, where wet microspheres instead of dry microspheres were used during loading. Under the same dry weight, wet microspheres can load more Doxo than dry microspheres (data not shown) due to the less swelling of the dry microspheres in a Doxo solution compared to wet microspheres that were fully swollen in normal saline (data not shown).

Table 1
Various batches of OCMC/CCN microspheres.

Microspheres	OCMC	Mean diameter (μm)	Swelling ratio, q	Degradation (day)	Doxo loading (mg/mg wet microsphere)
MS-I	OCMC-I	540 ± 50	10.2	14	0.066
MS-II	OCMC-II	580 ± 60	8.8	29	0.075
MS-III	OCMC-III	830 ± 60	8	88	0.077

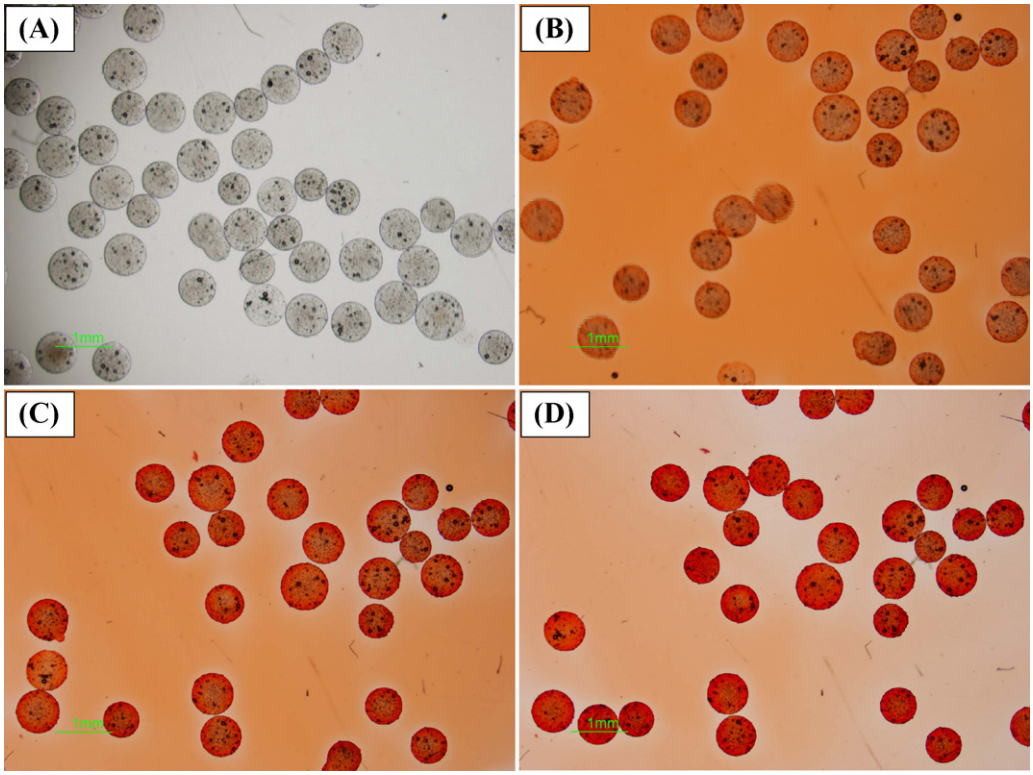

Fig. 2. Photomicrographs of MS-II before (A) and after uptake of Doxo over time 45 s (B), 10 min (C), and 30 min (D).

Doxo gives out red fluorescence under laser excitation, which allows for the detection of the drug in delivery systems such as liposomes (Kim and Wainer, 2010), micelles (Hu et al., 2009) or microspheres (Gonzalez et al., 2008). The loading of Doxo was therefore further confirmed with a fluorescence microscope. As shown in Fig. 4A, loaded microspheres exhibit red color and round shape under fluorescence microscope. Fig. 4B depicts the fluorescence intensity across the surface of a loaded microsphere. The curve shows that fluorescence intensity is relatively even across the surface, indicating an even distribution of loaded Doxo on the surface of the microsphere.

Internal Doxo distribution of the microspheres was investigated with confocal microscopy. Fig. 5 presents a series of confocal images from top of a microsphere downward throughout its structure at 20 μm intervals. The intensity of the images correlates to the concentration of Doxo loaded. Image of Fig. 5A shows the outer layer of the microsphere, which has a homogeneous fluorescence distribution. As sections moved down (Fig. 5B–F), the center of the image gradually became less intense although there was still Doxo present. The fluorescence was found to be concentrated in the outer 20 ± 5 μm layer of the microsphere, indicating the Doxo loaded is mainly distributed in the outer layer of the microsphere.

3.3. Release of Doxo from the microspheres

Similar to the Doxo loading above, Doxo release was monitored spectrophotometrically with the UV–vis spectrometer. Doxo released from the loaded microspheres shows a nearly identical UV–vis absorption spectrum with that of free Doxo (data not shown), indicating there is no adverse effect of the loading and releasing on the structure integrity of the Doxo (Liu et al., 2001). Doxo release has been performed both with refreshing medium and without refreshing medium. In the absence of medium refreshing, the releasing was conducted in 0.9% normal saline (pH = 6), 0.01 M PBS (pH = 7.4), 0.5 M acetate buffer (pH = 5.2), and distilled water, respectively. Evidently, the release of the Doxo loaded OCMC/CCN microspheres was affected strongly by the pH value, ion strength and degree of crosslinking.

Fig. 6A illustrates Doxo release profiles from MS-II (totally 0.23 mg Doxo loaded) in 2 mL normal saline, PBS and acetate buffer. There is a burst release in the beginning. At 48 h, Doxo concentrations in the releasing medium are 0.04, 0.027, 0.023 mg/mL (corresponding to 34.7%, 23.5%, and 19.6% of the total Doxo loaded) in normal saline, acetate buffer and PBS, respectively. In normal saline, Doxo was saturated in 2 weeks when the medium was not replaced. In PBS, Doxo release reached its equilibrium state in 2 days. However, in acetate buffer (pH = 5.2), the increase in the concentration of Doxo in the releasing medium was observed over 20 days. Schiff bases are well known to be biodegradable via hydrolysis, and the stability of these bonds decreases as the pH value decreases. As a result, the ion change is faster while the Schiff base in the microspheres was subject to hydrolysis in a lower pH value. This is visually evidenced by the decrease of the amount of beads in the medium (data not shown). Tumor is well known to be acidic (Saito and Hoffman, 2007). Therefore, it is speculated that the OCMC/CCN microspheres will release more Doxo in the tumor bed, which would be very promising for chemoembolotherapy.

In distilled water, there is no ion for ion exchange with Doxo. As expected, the Doxo release from MS-II in distilled water reaches its equilibrium state very shortly and the total amount released is 0.0024 mg (about 0.65% of total Doxo loaded in the microspheres), which is much lower compared to that in normal saline or acetate buffer (Fig. 6B). It is worth noting that the microspheres were not washed after taken out of the loading solution (the liquid was removed as much as possible by a pipette). Therefore, the little amount of Doxo released in water is the (unbinded) Doxo attached to the surface of the microspheres. This phenomenon was also observed during the releasing process of DC beads in water (Gonzalez et al., 2008). To further confirm the key role of the ions during the release, the releasing medium was replaced by nor-

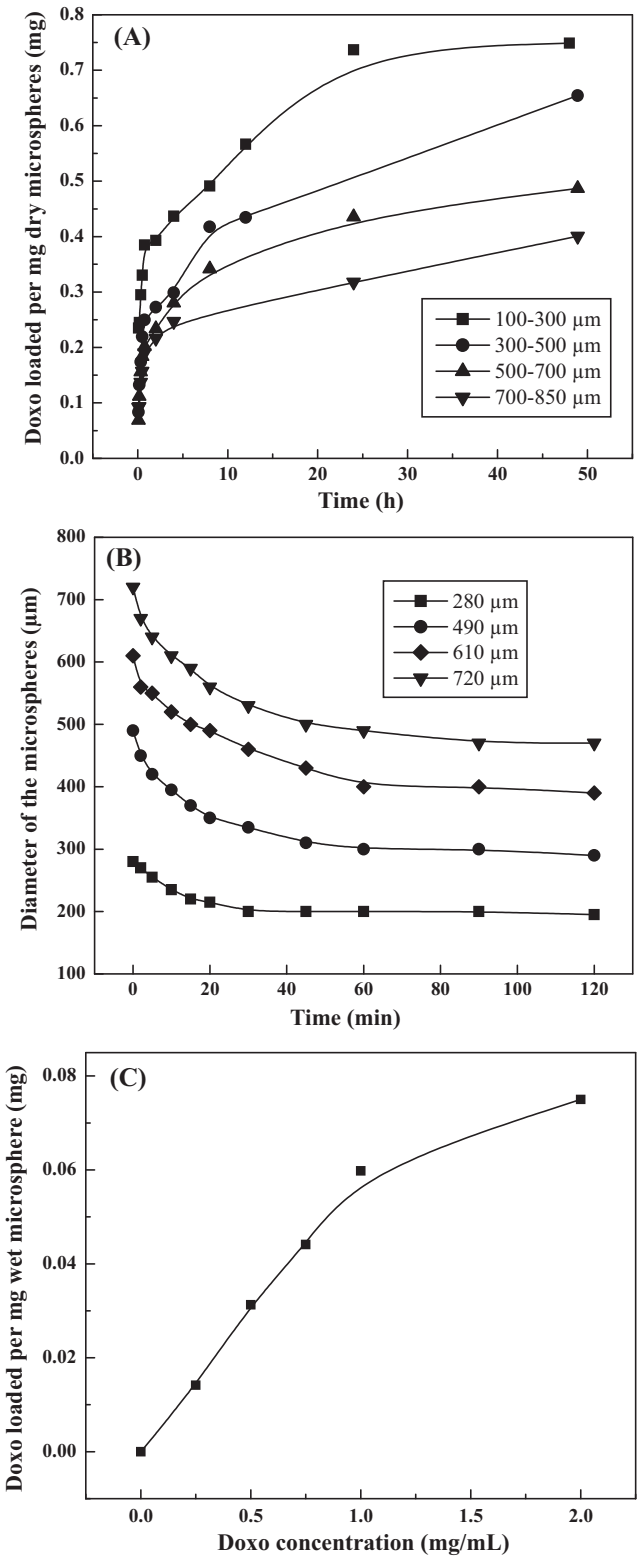

Fig. 3. (A) Loading dynamics of the MS-II in size range of 100–300, 300–500, 500–700, 700–850 μm in a 2 mg/mL Doxo solution; (B) dependence of the MS-II size in Doxo on the loading time; (C) dependence of the Doxo loading amount on the concentration Doxo solution.

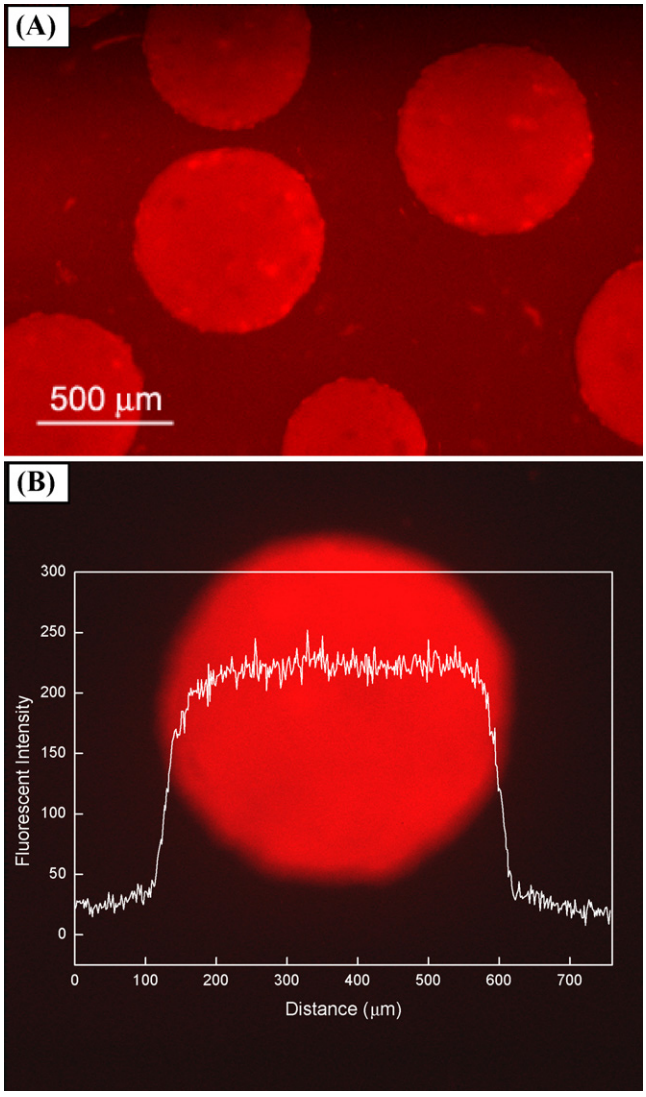

Fig. 4. Fluorescent microscopy image (A) and fluorescent intensity across the surface (B) of Doxo loaded microspheres.

mal saline after the Doxo release of the microspheres reached its equilibrium state in distilled water. As shown in Fig. 6B, the microspheres started to release Doxo rapidly, which is attributed to the presence of Na^+ in the releasing medium. Fig. 6C depicts the influence of temperature on Doxo release. Compared to results at 22 °C, Doxo release at 37 °C was faster in the beginning and the total amount of Doxo loaded was higher whereas their release patterns were similar, which is likely attributable to the fact that at higher temperature, the drug diffusion from the microspheres into the release medium is faster.

Fig. 6 D shows the Doxo released from MS-II microspheres and DC beads in size range of 300–500 μm in PBS. Both beads exhibit a rapid release followed by a plateau. However, the rate of Doxo release from MS-II is slower than that from DC beads. For instance, after 7 h, Doxo released from loaded MS-II and loaded DC beads were 6% and 10%, respectively. Although both types of microspheres can load Doxo through the ion-exchange mechanism, the ions involved are different. DC beads contain sulfonic groups while OCMC/CCN microspheres contain carboxylic groups. As mentioned above in Fig. 3B, the microspheres shrink while taking up Doxo and the percentage of shrinkage is slightly higher than DC beads in the same size range (Lewis et al., 2007). Hence, it is speculated that the stacking density of Doxo and the relative crosslinking density of the microsphere matrix in OCMC/CCN microspheres is relatively higher compared to that of DC beads, resulting in a larger steric hindrance for drug release.

To clarify the effect of the composition of the microspheres on the Doxo release, the Doxo release from MS-I, MS-II, and MS-

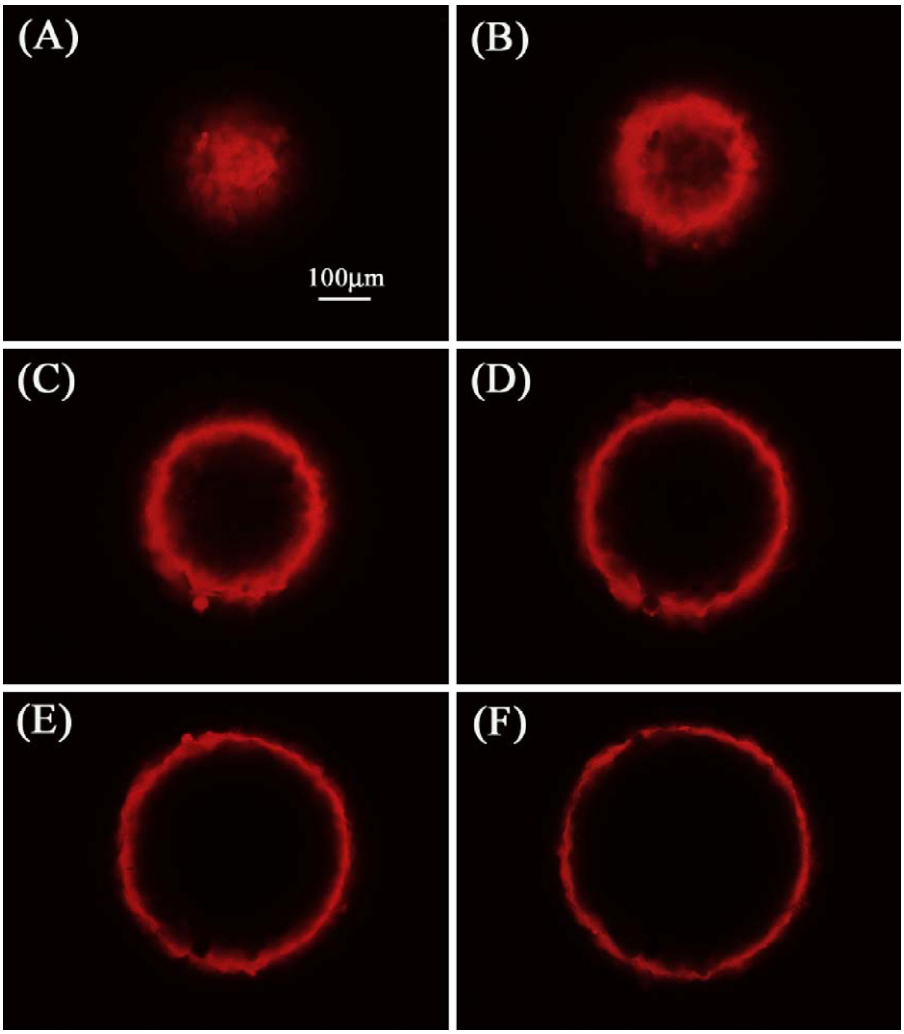

Fig. 5. Confocal laser scanning microscopy images of Doxo loaded MS-II microspheres showing progressive sections from outside inwards at 20 μm intervals (A)–(F).

III microspheres (300–500 μm) was carried out in normal saline. As depicted in Fig. 7, with an increase in the targeted oxidation degree from 10% to 50% in OCMC, corresponding to an increase in the targeted crosslinking degrees of the microspheres, the initial Doxo release speed significantly decreased. Around 6 days, the release of all three microspheres reaches a plateau, indicating no more Doxo will be released from the microspheres if the medium is changed due to the equilibrium state between Doxo in the releasing medium and in the microspheres. In addition, the final Doxo released was also strongly affected by the degree of polymer crosslinking (Fig. 7). At 2 weeks, the final concentrations of Doxo released from MS-I, MS-II and MS-III in the medium are 0.077, 0.055 and 0.045 mg/mL, respectively. The higher the oxidation degree, the higher the crosslinking density. As shown in Table 1, the swelling ratio of OCMC/CCN microspheres decreased in the sequence of MS-I > MS-II > MS-III. Therefore, compared to MS-I and MS-II, it is more difficult for Doxo molecules to diffuse into the microspheres. In other words, it will take longer for the microspheres with higher crosslinking density to load Doxo. Correspondingly, the release of the Doxo from MS-III microspheres will be slower and the total Doxo released will be lower.

Table 2
Release constants (k) and diffusion exponents (n) of Doxo loaded OCMC/CCN microspheres in a 0.9% NaCl aqueous solution.

Microspheres	k	n	r^2
MS-I	0.042	0.56	0.9970
MS-II	0.031	0.55	0.9967
MS-III	0.027	0.59	0.9917

In order to understand the nature of Doxo release from OCMC/CCN microspheres, the release data were also analyzed with an empirical equation:

$$\frac{M_t}{M_\infty} = kt^n \quad (2)$$

where M_t/M_∞ is the fraction of drug released, k is the release kinetic parameter, and n is the diffusional exponent, which indicates the transport mechanism. For a Fickian diffusion, n is equal to 0.5. For a non-Fickian diffusion, n takes values higher than 0.5. The case of anomalous diffusion with $n = 1$ is known as Case II transport (Peppas and Franson, 1983). For the drug release of MS-I, MS-II, and MS-III microspheres in normal saline, $\ln(M_t/M_\infty)$ versus $\ln t$ graphs are plotted and representative k and n are calculated from the slopes and intercepts of the lines, respectively, and are presented in Table 2. Values of k decreases with increasing crosslinking density while they are small in the range between 0.027 and 0.042, suggesting a mild type of interactions between Doxo and the microsphere matrices (Karadag et al., 2005). On the other hand, n varies from 0.55 to 0.59, which is over 0.5. Therefore, the drug release mechanism of the OCMC/CCN microspheres follows a non-Fickian behavior (Peppas and Franson, 1983; Rokhade et al., 2007).

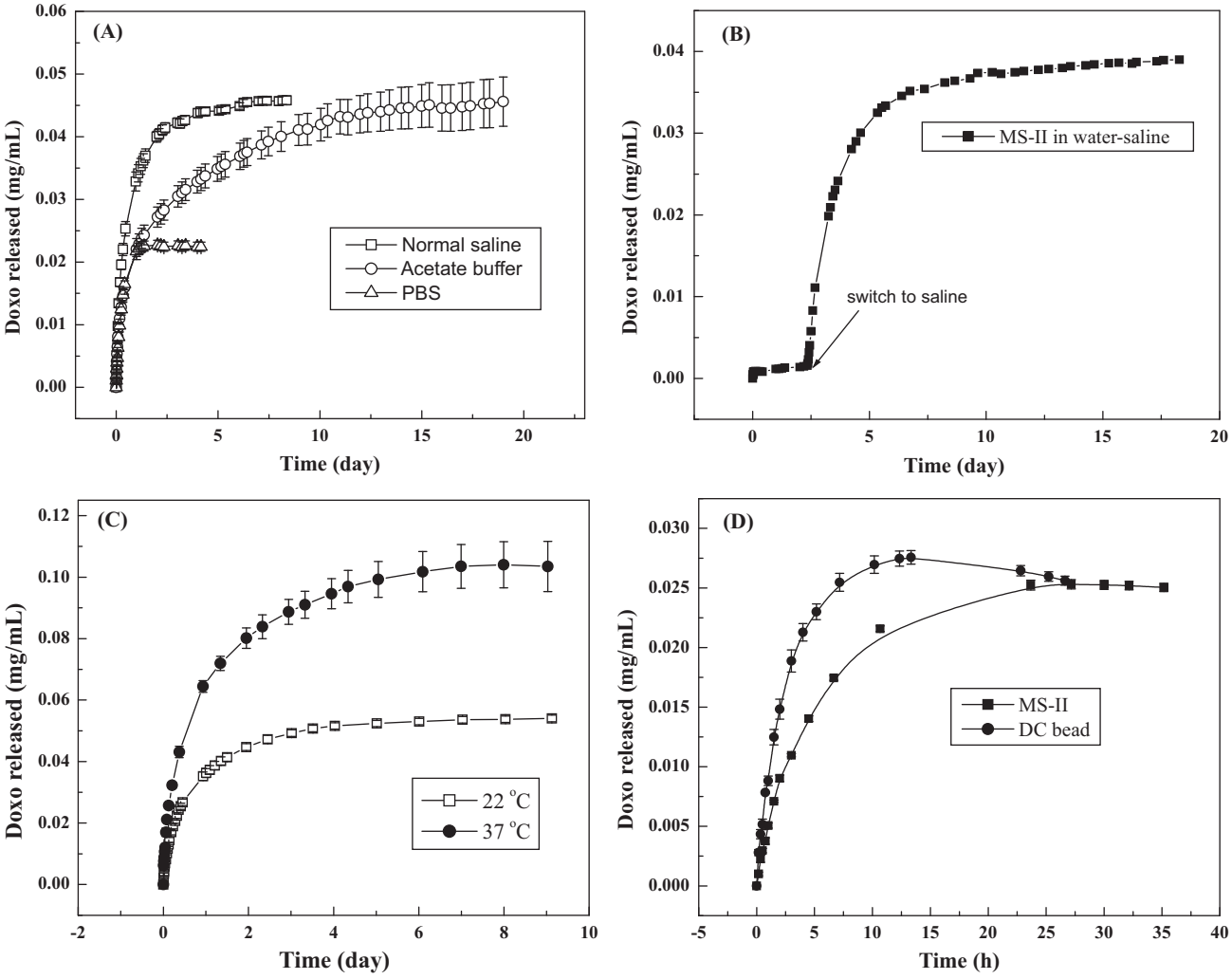

Fig. 6. (A) Doxo releasing from MS-II microspheres in 0.01 M PBS, 0.5 M acetate buffer, and normal saline without replacing the medium; (B) comparison of Doxo releasing from MS-II in distilled water and normal saline; (C) comparison of Doxo releasing from MS-II at 22 °C and 37 °C; (D) comparison of Doxo releasing in PBS from MS-II and DC beads.

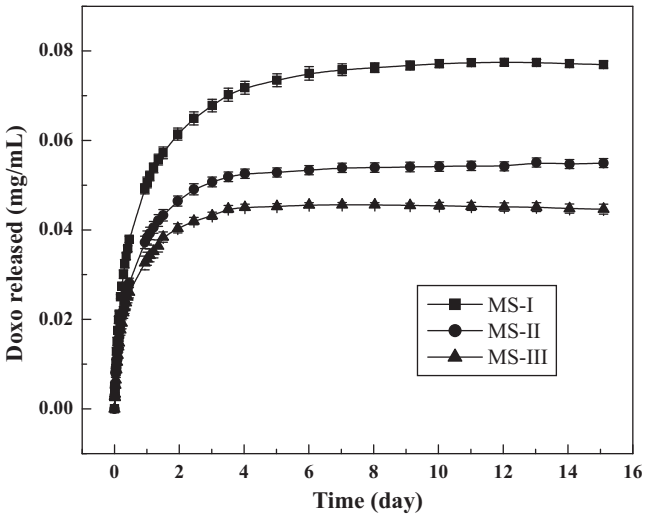

Fig. 7. Doxo releasing from MS-I, MS-II, and MS-III microspheres in normal saline.

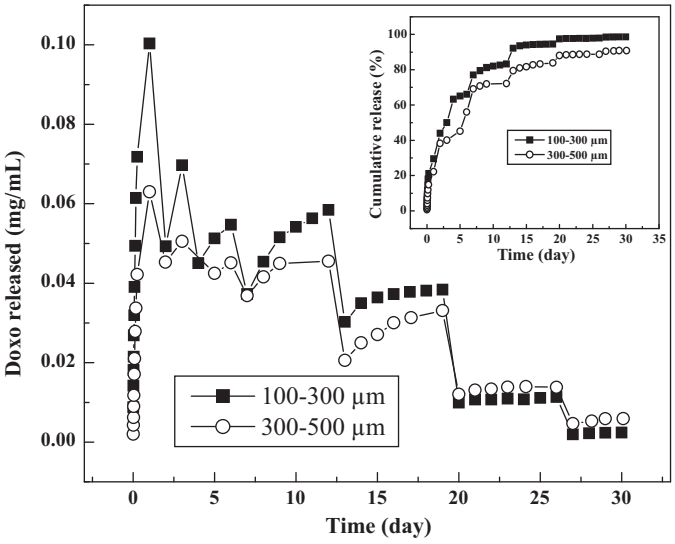

Fig. 8. Doxo releasing from 100 to 300 and 300 to 500 μm MS-II in normal saline with replacing the medium on day 1, 3, 6, 12, 19 and 26. Insert: cumulative release of Doxo from the microspheres.

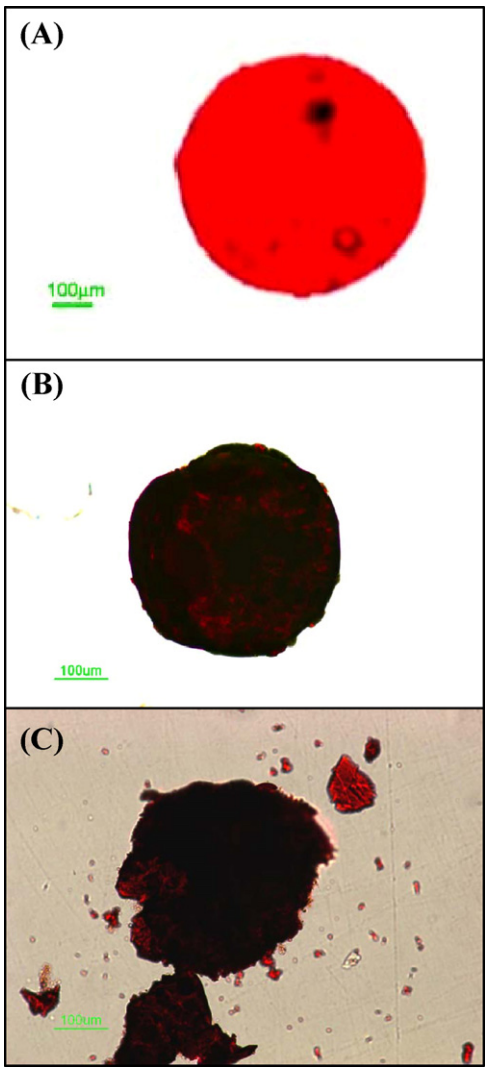

Fig. 9. Degradation of the Doxo loaded microspheres in 4 mg/mL lysozyme after (A) day 0, (B) 1.5 months, and (C) 3 months.

In the refreshing medium model, the release was carried out in normal saline only. Fig. 8 presents the time dependence of Doxo released from 100 to 300 and 300 to 500 μm of MS-II microspheres in normal saline. The releasing medium was changed on day 1, 3, 6, 12, 19, and 26. Smaller microspheres have a faster release rate, and both size-ranges of microspheres exhibit a peak at 24 h, where total amount of Doxo released from 100 to 300 μm microspheres (0.1 mg/mL) is higher than that from 300 to 500 μm microspheres (0.06 mg/mL). This is due to the larger surface area contacted with the normal saline for the smaller sizes of microspheres. Furthermore, for bigger microspheres, the distance for drug diffusion within the microspheres is longer (Taylor et al., 2007). After refreshing medium, loaded microspheres continued to release Doxo in the following days without changing medium, while the initial releasing speed decreased as times of refreshing medium increased. Smaller microspheres exhibit a shorter release period, and the total Doxo release can last about 1 month. At day 20, total Doxo released is 97% and 88% of total Doxo loaded for 100–300 μm and 300–500 μm microspheres (see the insert), respectively. After day 20, the drug release assumed a very slow pace. Altogether, the releasing of Doxo can be sustained for a long time because of OCMC/CCN microspheres' adsorption and physical trapping. It is speculated that the presence of the microspheres could decrease the systematic Doxo concentration and thus have the potential to reduce the side effect of Doxo. In addition, it was noted that during this study, even though the release was apparently stopped after 30 days, the drug was not 100% released out of the microspheres (see insert of Fig. 8), which is evidenced by the red color of the microspheres after releasing (data not shown).

3.4. Enzymatic degradation of the Doxo loaded microspheres

As the unloaded MS-II can be degraded by lysozyme within 1 month (Table 1), the loaded microspheres are expected to be degradable in the presence of lysozyme. Fig. 9 depicts the morphology change of Doxo loaded MS-II in a 4 mg/mL lysozyme solution. There was a considerable shrinkage when Doxo loaded microspheres were immersed in the lysozyme solution (Fig. 9B). The Doxo loaded microsphere degraded into pieces within 3 months (Fig. 9C), which is longer than the time needed for unloaded microspheres. As mentioned above (Fig. 3B), the size of the microsphere decreased after loading, indicating the crosslinking density per volume of the microsphere increased compared to original microspheres. As a result, the degradation time of the loaded microspheres is considerably longer than unloaded microspheres.

4. Conclusions

Bioresorbable OCMC/CCN microspheres have been prepared and evaluated as potential drug delivery carriers of an anticancer drug, doxorubicin. In vitro loading and releasing kinetics and mechanism have been determined, indicating that ion-exchange is the main mechanism dominating the release kinetics of the microspheres while the mass transport type is non-Fickian. Doxo loaded is distributed relatively even on the surface of the microspheres but concentrated mainly in the outer layer of the microspheres. Particularly, drug loading and releasing can be easily modulated by tuning the composition of hydrogel microspheres. Protonation of carboxylic groups in the microsphere matrix at acidic conditions resulted in an accelerated release of Doxo, which is desired for treating tumors. Therefore, we believe that the bioresorbable OCMC/CCN microspheres are very promising for chemoembolotherapy.

Acknowledgement

We thank Prof. Afishin A. Divani from Neurology Department, in University of Minnesota for his technical assistance.

Appendix A. Supplementary data

Supplementary data associated with this article can be found, in the online version, at doi:10.1016/j.ijpharm.2011.02.058.

References

Agnihotri, S.A., Aminabhavi, T.M., 2006. Novel interpenetrating network chitosan–poly(ethylene oxide-g-acrylamide) hydrogel microspheres for the controlled release of capecitabine. Int. J. Pharm. 324, 103–115.
Bibby, D.C., Talmadge, J.E., Dalal, M.K., Kurz, S.G., Chytil, K.M., Barry, S.E., Shand, D.G., Steiert, M., 2005. Pharmacokinetics and biodistribution of RGD-targeted doxorubicin-loaded nanoparticles in tumor-bearing mice. Int. J. Pharm. 293, 281–290.
Chen, X.G., Park, H.J., 2003. Chemical characteristics of O-carboxymethyl chitosans related to the preparation conditions. Carbohydr. Polym. 53, 355–359.
Cheung, R.Y., Kuba, R., Rauth, A.M., Wu, X.Y., 2004. A new approach to the in vivo and in vitro investigation of drug release from locoregionally delivered microspheres. J. Control. Release 100, 121–133.
Dreis, S., Rothweiler, F., Michaelis, M., Cinatl Jr., J., Kreuter, J., Langer, K., 2007. Preparation, characterization and maintenance of drug efficacy of doxorubicin-loaded human serum albumin (HSA) nanoparticles. Int. J. Pharm. 341, 207–214.
Greenwald, R.B., Choe, Y.H., McGuire, J., Conover, C.D., 2003. Effective drug delivery by PEGylated drug conjugates. Adv. Drug Deliv. Rev. 55, 217–250.

Gonzalez, M.V., Tang, Y., Phillips, G.J., Lloyd, A.W., Hall, B., Stratford, P.W., Lewis, A.L., 2008. Doxorubicin eluting beads—2: methods for evaluating drug elution and in-vitro:in-vivo correlation. J. Mater. Sci.: Mater. Med. 19, 767–775.

Guhagarkar, S.A., Gaikwad, R.V., Samad, A., Malshe, V.C., Devarajan, P.V., 2010. Polyethylene sebacate–doxorubicin nanoparticles for hepatic targeting. Int. J. Pharm. 401, 113–122.

Hruby, M., Konak, C., Ulbrich, K., 2005. Polymer micellar pH-sensitive drug delivery system for doxorubicin. J. Control. Release 103, 137–148.

Hu, F.Q., Liu, L.N., Du, Y.Z., Yuan, H., 2009. Synthesis and antitumor activity of doxorubicin conjugated stearic acid-g-chitosan oligosaccharide polymeric micelles. Biomaterials 30, 6955–6963.

Ito, T., Yeo, Y., Highley, C.B., Bellas, E., Benitez, C.A., Kohane, D.S., 2007. The prevention of peritoneal adhesions by in situ cross-linking hydrogels of hyaluronic acid and cellulose derivatives. Biomaterials 28, 975–983.

Karadag, E., Uzum, O.B., Saraydin, D., Guven, O., 2005. Dynamic swelling behavior of radiation induced polyelectrolyte poly(AAm-co-CA) hydrogels in urea solutions. Int. J. Pharm. 301, 102–111.

Karki, S.B., Ostovi, D., 2004. Assessing aggregation of peptide conjugate of doxorubicin using quasi-elastic light scattering and 600 MHz NMR. Int. J. Pharm. 271, 181–187.

Kettenbach, J., Stadler, A., Katzler, I.V., Schernthaner, R., Blum, M., Lammer, J., Rand, T., 2008. Drug-loaded microspheres for the treatment of liver cancer: review of current results. Cardiovasc. Intervent. Radiol. 31, 468–476.

Kim, J.O., Kabanov, A.V., Bronich, T.K., 2009. Polymer micelles with crosslinked polyanion core for delivery of a cationic drug doxorubicin. J. Control. Release 138, 197–204.

Kim, H.S., Wainer, I.W., 2010. Simultaneous analysis of liposomal doxorubicin and doxorubicin using capillary electrophoresis and laser induced fluorescence. J. Pharm. Biomed. Anal. 52, 372–376.

Kim, T.H., Mount, C.W., Gombotz, W.R., Pun, S.H., 2010. The delivery of doxorubicin to 3-D multicellular spheroids and tumors in a murine xenograft model using tumor-penetrating triblock polymeric micelles. Biomaterials 31, 7386–7397.

Lee, K.H., Liapi, E.A., Cornell, C., Buijs, P.R.M., Vossen, J.A., Ventura, V.P., Geschwind, J.F.H., 2010. Doxorubicin-loaded quadrasphere microspheres: plasma pharmacokinetics and intratumoral drug concentration in an animal model of liver cancer. Cardiovasc. Interv. Radiol. 33, 576–582.

Lewis, A.L., Gonzalez, M.V., Leppard, S.W., Brown, J.E., Stratford, P.W., Phillips, G.J., Lloyd, A.W., 2007. Doxorubicin eluting beads-1: effects of drug loading on bead characteristic and drug distribution. J. Mater. Sci.: Mater. Med. 18, 1691–1699.

Lewis, A.L., Taylor, R.R., Hall, B., Gonzalez, M.V., Willis, S.L., Stratford, P.W., 2006. Pharmacokinetic and safety study of doxo-eluting beads in a porcine model of hepatic arterial embolization. J. Vasc. Interv. Radiol. 17, 1335–1343.

Liu, Z., Cheung, R., Wu, X.Y., Ballinger, J.R., Bendayan, R., Rauth, A.M., 2001. A study of doxorubicin loading onto and release from sulfopropyl dextran ion-exchange microspheres. J. Control. Release 77, 213–224.

Parkin, D.M., Bray, F., Ferlay, J., Pisani, P., 2005. Global cancer statistics, 2002. CA Cancer J. Clin. 55, 74–108.

Peppas, N.A., Franson, N.M., 1983. The swelling interface number as a criterion for prediction of diffusional solute release mechanisms in swellable polymers. J. Polym. Sci. 21, 983–997.

Qia, J., Yao, P., Heb, F., Yub, C., Huang, C., 2010. Nanoparticles with dextran/chitosan shell and BSA/chitosan core—doxorubicin loading and delivery. Int. J. Pharm. 393, 176–184.

Rokhade, A.P., Patil, S.A., Aminabhavi, T.M., 2007. Synthesis and characterization of semi-interpenetrating polymer network microspheres of acrylamide grafted dextran and chitosan for controlled release of acyclovir. Carbohydr. Polym. 67, 605–613.

Saito, H., Hoffman, A.S., 2007. Delivery of doxorubicin from biodegradable PEG hydrogels having Schiff base linkages. J. Bioact. Compat. Polym. 22, 589–601.

Tan, E.C., Lin, R., Wang, C.H., 2005. Fabrication of double-walled microspheres for the sustained release of doxorubicin. J. Colloid Interface Sci. 291, 135–143.

Taylor, R.R., Tang, Y., Gonzalez, M.V., Stratford, P.W., Lewis, A.L., 2007. Irinotecan drug eluting beads for use in chemoembolization: in vitro and in vivo evaluation of drug release properties. Eur. J. Pharm. Sci. 30, 7–14.

Tsochatzis, E.A., Germani, G., Burroughs, A.K., 2010. Transarterial chemoembolization, transarterial chemotherapy, and intra-arterial chemotherapy for hepatocellular carcinoma treatment. Semin. Oncol. 37, 89–93.

Vinchon-Petit, S., Jarnet, D., Michalak, S., Lewis, A., Benoit, J.P., Menei, P., 2010. Local implantation of doxorubicin drug eluting beads in rat glioma. Int. J. Pharm 402, 184–189.

Weng, L., Le, H., Golzarian, J., 2010. Abstract No 94: new bioresorbable hydrogel microspheres for therapeutic embolization: development and in vitro evaluation. J. Vasc. Interv. Radiol. 21, S37.

Ye, Y.Q., Yang, F.L., Hu, F.Q., Du, Y.Z., Yuan, H., Yu, H.Y., 2008. Core-modified chitosan-based polymeric micelles for controlled release of doxorubicin. Int. J. Pharm. 352, 294–301.